

Determination of Protein Aggregation With Differential Mobility Analysis: Application to IgG Antibody

Leonard F. Pease III,¹ John T. Elliott,¹ De-Hao Tsai,¹ Michael R. Zachariah,^{1,2} Michael J. Tarlov¹

¹National Institute of Standards and Technology (NIST), 100 Bureau Drive MS 8362, Gaithersburg, Maryland 20899; telephone: 301-975-2058 (M.J.T.)/301-405-4311 (M.R.Z.); fax: 301-975-2643 (M.J.T./M.R.Z.); e-mail: mrz@umd.edu; mtarlov@nist.gov

²University of Maryland, College Park, Maryland 20742

Received 24 March 2008; revision received 15 May 2008; accepted 16 May 2008

Published online 16 June 2008 in Wiley InterScience (www.interscience.wiley.com). DOI 10.1002/bit.22017

ABSTRACT: Here we describe the use of electrospray differential mobility analysis (ES-DMA), also known as gas-phase electrophoretic mobility molecular analysis (GEMMA), as a method for measuring low-order soluble aggregates of proteins in solution. We demonstrate proof of concept with IgG antibodies. In ES-DMA, aqueous solutions of the antibody protein are electrosprayed and the various aerosolized species are separated according to their electrophoretic mobility using a differential mobility analyzer. In this way, complete size distributions of protein species present from 3 to 250 nm can be obtained with the current set up, including distinct peaks for IgG monomers to pentamers. The sizes of the IgG and IgG aggregates measured by DMA were found to be in good agreement with those calculated from simple models, which take the structural dimensions of IgG from protein crystallographic data. The dependence of IgG aggregation on the solution concentration and ionic strength was also examined, and the portion of aggregates containing chemically crosslinked antibodies was quantified. These results indicate that ES-DMA holds potential as a measurement tool to study protein aggregation phenomena such as those associated with antibody reagent manufacturing and protein therapeutics.

Biotechnol. Bioeng. 2008;101: 1214–1222.

© 2008 Wiley Periodicals, Inc.

KEYWORDS: antibody aggregation; protein crystallography structure; differential mobility analysis (DMA); electrospray (ES); irreversible aggregation

industry (Jimenez et al., 2007; Minton, 2007). Protein drug products can be exposed to conditions that alter their chemical and physical stability, resulting in aggregation or precipitation during cell culture, purification, formulation, or filling. These aggregates can have unpredictable consequences on drug dose and biological activity of a therapeutic protein. Likely the most serious concern is that aggregates can trigger a severe, or even life threatening, immune response in patients (Braun et al., 1997; Demeule et al., 2007; Frokjaer and Otzen, 2005; Hermeling et al., 2004; Mauro et al., 2007; Treuheit et al., 2002; Wang, 2005). For these reasons, protein therapeutics must be extensively characterized for aggregation as part of the quality assurance/control process for obtaining regulatory approval.

A variety of techniques are used to ascertain aggregation of protein preparations including analytical ultracentrifugation, field flow fractionation, size exclusion chromatography with UV-vis detection, and dynamic light scattering (Attri and Minton, 2005; Bondos, 2006; Wang, 2005). Here we report on an alternative means of measuring aggregation, electrospray-differential mobility analysis (ES-DMA), also known as gas-phase electrophoretic mobility molecular analysis (GEMMA; Bacher et al., 2001; Kaufman, 2000; Knutson and Whitby, 1975). As will be shown, ES-DMA offers the ability to easily detect aggregates up to 250 nm in size and smaller aggregates down to 3 nm with monomeric resolution. This enables characterization of the initial states of aggregation, particularly the dimers, trimers, and tetramers.

ES-DMA is conceptually similar to mass spectrometry (MS), but it differs from ES-MS in several ways. First, because the DMA operates at atmospheric pressure, protein species are subject to aerodynamic drag. The instrument accordingly separates proteins based on their charge-to-aerodynamic size ratio (i.e., electrical mobility) as opposed to the charge-to-mass ratio (Knutson and Whitby, 1975). Second, electrosprayed ions pass through a neutralizing

Introduction

Protein aggregation is a major concern in the production of recombinant protein therapeutics by the biotechnology

Reference to commercial equipment, supplies, or software neither implies its endorsement by the National Institute of Standards and Technology (NIST) nor implies it to be necessarily best suited for this purpose.

Correspondence to: M.R. Zachariah and M.J. Tarlov

chamber to reduce the charge on each droplet to +1, 0, or -1 (Bacher et al., 2001). Thus, the effective diameter of the particle may be determined directly. Third, ES-DMA can characterize species with molecular weights greatly exceeding 10 kDa, which makes it well suited for characterizing larger protein aggregates. The particular instrument used in these studies can measure proteins with electrical mobility diameters up to 120 nm or approximately 400 MDa (Bacher et al., 2001).

In this article we describe methods for analyzing ES-DMA spectra to obtain protein aggregate sizes and distributions. We chose IgG antibodies as a model protein system for these studies because they represent a commercially important class of therapeutic proteins. Monoclonal antibodies comprise half of the top 10 biologicals marketed in 2006, and over 150 are advancing through clinical trials, making them a commercially compelling class of proteins (La Merie Business Intelligence, February 2007). Bacher et al. were the first to apply ES-DMA to the study of protein aggregation by demonstrating the ability to detect monomers, dimers, and trimers of bovine IgG antibodies. They reported that heavy and light chains of IgG could be distinguished following denaturation and chemical cleavage of disulfide bridges. In addition, mobility sizes measured for various proteins were correlated with protein molecular weight. Here we build on this earlier work by elucidating the conditions under which ES-DMA can reliably determine the aggregation of human IgG. We demonstrate that protein and protein aggregate peaks can be unambiguously assigned using simple structural models that are derived from both exacting protein crystallographic structures and simpler approximations of protein structure. Using ES-DMA, we specifically examine the effects of protein concentration, ionic strength, and pH on the formation of reversible (physically) and irreversible (chemically) aggregates of IgG. This study represents the first rigorous, systematic study of ES-DMA as applied to the problem of protein aggregation.

Materials and Methods

Solutions containing IgG antibodies were electrosprayed (TSI, Inc., Shore View, MN, #3480) to produce a narrow distribution of droplet diameters (Kaufman, 2000). Aerosolized droplets were produced only under conditions where a stable cone-jet meniscus at the tip of a 25 μm inner diameter capillary was visually observed, although there was some variability in the current within a give sample run ($V = 1.40\text{--}3.03$ kV, $I = -19$ to -411 nA). Immediately downstream of the ES, droplets were passed through a neutralizing chamber containing a Po-210 ionizing radiation source from which a majority of droplets emerge with a charge of +1, 0, or -1. As the droplets evaporated, this charge remained on the dried proteins. These proteins pass into the differential mobility analyzer (DMA; TSI, Inc., #3080). The DMA acts like an ion-mobility band-pass filter that for a given electrode voltage and gas flow rate enables a narrow size band of ions to be sent to the condensation

particle counter (CPC), which measures the number concentration of particles in the gas (TSI, Inc., #3025A). In this manner proteins with diameters greater than 3 nm can be sized. The sampling and DMA sheath flow rates were 1.2 and 30 L/min, respectively. The conversion from voltage to mobility size has been described in detail elsewhere (Mulholland et al., 2006; Pease et al., 2007). Because we apply a negative bias to ions within the DMA, only proteins that acquire a positive charge are detected. The fraction of proteins emerging with a positive charge is size dependent. A modified expression for the Boltzmann distribution (Wiedensohler, 1988) was used to correct for this effect, transforming the distribution of positively charged proteins into the complete distribution of all proteins regardless of charge (Pease et al., 2007).

We note that electrospray is remarkably gentle (Loo, 1997). Bacher et al. (2001) examined several multimeric proteins (including streptavidin, avidin, alcohol dehydrogenase, and catalase) and found that these noncovalently bound complexes do not breakup within a normal pH range (pH 4.5–8.5). Only under stressful conditions (e.g., streptavidin heated for 30 min to 80°C at pH 0.8) were peaks corresponding to fragments observed in the ES-DMA spectra. Thus, electrospray systems like ours tend to preserve noncovalently bound aggregates.

The size of the initial electrosprayed droplets prior to evaporation was estimated by spraying a sucrose solution of known concentration and measuring the size of the remnant particle after solvent evaporation. Three microliters of a 4.85% (v/v) sucrose solution was added to 97.0 μL of 2.0 or 20 mmol/L ammonium acetate. The surface tension of these solutions was comparable to antibody containing solutions prepared in the same amount and concentration of ammonium acetate as determined by contact angle measurements of solutions on a silicon substrate in air; corresponding samples differed by less than 3°.

For these studies, polyclonal rabbit antibodies specific to the bacteriophage MS2 with a concentration of 2.8 mg/mL were obtained from Tetracore (Rockville, MD, product #TC-7004). The as-received solutions contained significant amounts of nonvolatile salts. The presence of high salt concentrations can interfere with the ES-DMA measurement in two ways. First, the evaporation of electrosprayed droplets containing high salt concentrations results in the formation of salt particles whose signal can overlap that of the antibody or other analytes of interest. Second, the salts can precipitate out on the surface of the antibody, encrusting it. The apparent size of these encrusted antibodies measured by the DMA then exceeds the actual size. Therefore, nonvolatile salts must be removed or largely reduced. We accomplished this by dialyzing 150 μL of as-received antibodies with a slide-a-lyzer cartridge (Pierce, Rockford, IL) having a 10 kDa cutoff for 18 h in a 20 mmol/L ammonium acetate solution at pH 8. All ammonium acetate solutions were prepared using deionized water (>18.0 M Ω cm) and adjusting the pH to 8.0 (with either glacial acetic acid (Mallinckrodt, Phillipsburg, NJ) or ammonium hydroxide

(Baker, Phillipsburg, NJ, #9721-01)). Upon removal of the antibodies from the dialysis cartridge, the volume had increased to 230 μL . These antibodies were further diluted into ammonium acetate of the concentration and pH specified in the figure captions. Low protein binding microcentrifuge tubes (Eppendorf, Westbury, NY) were used to prevent antibody adsorption to the sidewalls. Solutions to examine the effect of pH were prepared by adding 25.0 or 125 μL of glacial acetic acid or 50.0 μL of 30% (by weight) ammonium hydroxide and raising the volume to 1.00 mL with ammonium acetate solution of the specified concentration. The samples were maintained at 4°C until use.

Chemically crosslinked aggregates (i.e., those held together by chemical bonding as opposed to weaker physical forces) were prepared as follows. Paraformaldehyde (16% v/v) and glutaraldehyde (25% v/v) were obtained from Electron Microscopy Sciences (Hatfield, PA). Lyophilized human IgG antibody (Sigma, St. Louis, MO, #I4506) was dissolved in PBS (4.5 mg/mL), and aliquoted (200 μL) into microcentrifuge tubes. Water as a control (10 μL), formaldehyde (1 and 10 μL) or glutaraldehyde (1 and 10 μL) were added to separate aliquots. The samples were mixed and kept at room temperature for 10 min. White aggregates were observed in the 10 μL glutaraldehyde sample. Dialysis buffer, 2 mmol/L ammonium acetate, pH 8.5 (800 μL), was added to each aliquot, the aliquots were centrifuged (10,000g, 1 min), and the supernatant was collected into dialysis tubing (17,000 MWCO, SpectraPor, Houston, TX). The samples were dialyzed overnight in 2.0 L of 2.0 mmol/L ammonium acetate, pH 8.5. The dialyzed samples were collected and kept at 4°C until use. The final concentration of antibody in solution was approximately 1.5 $\mu\text{mol/L}$. Samples were further diluted to concentrations noted in the figure captions with ammonium acetate buffer.

To assign the peaks in the mobility spectra corresponding to each aggregate species or n-mer, the sizes of IgG aggregates were calculated in Mathematica using structural information from the protein databank. The atomic coordinates for all 10,400 atoms were obtained from the file IGG1-ALL.PDB (Padlan, 1994). Since the DMA selects particles on the basis of their aerodynamic drag, which is proportional to the projected area of the protein, projections of the proteins were obtained by confirming that the molecule was aligned with the x , y , and z axes (rotating if necessary) and then deleting one of the dimensions (e.g., z coordinates to obtain the x - y coordinates for the projection onto the x - y plane). As real atoms have a finite size, an average van der Waals (vdw) diameter, d_{vdw} , was obtained by weighting it by the number of each atomic species in the antibody with

$$d_{\text{vdw}} = 2 \left[\frac{\sum_{i=1}^5 \sum_{j=1}^{20} r_i^2 N_j M_{ij}}{\sum_{i=1}^5 \sum_{j=1}^{20} N_j M_{ij}} \right]^{1/2} \quad (1)$$

where i denotes one of the five atoms of carbon, hydrogen, oxygen, nitrogen, or sulfur, r_i is the van der Waals radius of atom i , N_j is the number of proteins of type j listed in the FASTA corresponding to IGG1-ALL.PDB, and M_{ij} represents the number of atoms of type i in protein j (Padlan, 1994). Each atom in the antibody's crystal structure with its finite size (i.e., d_{vdw} here at 2.8 Å) was sequentially projected onto a grid composed of 0.5 Å by 0.5 Å pixels. Each pixel with a nonzero value represents area occupied by at least one atom somewhere perpendicular to the plane of the projection. If more than one atom projects onto the same pixel, the pixel may accumulate a value greater than unity. The double counting problem was avoided, however, by counting the number of nonzero pixels and then multiplying the number of occupied pixels by the area of a pixel to yield the projected area. The process was repeated for each of the three projections yielding A_{front} , A_{side} , and A_{top} . Alternate calculation approaches that consider only the external atoms are computationally equivalent. The size of the antibody was then calculated as given below (see Eq. 2).

The size of aggregates or half antibodies were determined by essentially stacking one antibody in front of another. The size of the aggregated antibodies was predicted with projected areas $A'_{\text{front}} = A_{\text{front}}$, $A'_{\text{side}} = nA_{\text{top}}$, and $A'_{\text{top}} = nA_{\text{top}}$, where n is the number of antibodies in the aggregate. The size of the half aggregate was determined by $A'_{\text{front}} = A_{\text{front}}/2$, $A'_{\text{side}} = A_{\text{side}}$, and $A'_{\text{top}}/2$.

Results and Discussion

Here we use ES-DMA to examine both physical and chemical aggregation of polyclonal antibodies. Physical aggregates, also known as reversible aggregates, are held together by van der Waals forces or ionic attraction and may break up under shear forces, whereas chemical or irreversible aggregates are stable to shear due to their stronger chemical bonding. In the remainder of this article, we describe how peaks in ES-DMA spectra are identified. We then examine how protein concentration, ionic strength, solution pH, and electrospray droplet size affect the aggregation states. We also demonstrate the value of ES-DMA for analysis of irreversible aggregates by examining chemically crosslinked antibodies.

Rigorous Peak Identification

Figure 1 shows typical ES-DMA spectra acquired from sample solutions containing rabbit (Fig. 1a) and human (Fig. 1b) IgGs. The relatively simple spectrum for the rabbit IgG is dominated by a large peak at 8.6 nm with a peak of much lower intensity appearing at 10.7 nm. In contrast, the spectrum of the human IgG is more complex with the most intense peak observed at 9.4 nm along with at least 5 peaks appearing at higher mobility sizes. The peaks at 8.6 nm for the rabbit IgG in Figure 1a and 9.4 for the human IgG in Figure 1b are assigned to individual, intact antibodies. These

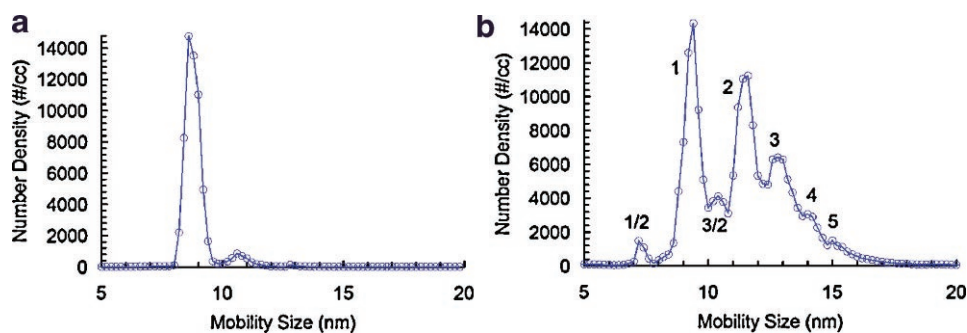


Figure 1. Typical ES-DMA spectra where number density is plotted versus the mobility size in nm for (a) rabbit IgG at 18 $\mu\text{g/mL}$ (120 nmol/L or 7.3×10^{13} antibodies/mL) in 20 mmol/L ammonium acetate, pH 8 and (b) human IgG previously lyophilized at approximately 75 $\mu\text{g/mL}$ (500 nmol/L or 3.0×10^{14} antibodies/mL) in 2.0 mmol/L ammonium acetate, pH 8.

mobility sizes represent the diameter of an equivalent sphere, exhibiting the same aerodynamic drag and charge as the antibody (i.e., electrical mobility). These sizes for human and rabbit IgG are similar to that for bovine IgG reported by Bacher et al. (2001) of 9.3 nm using ES-DMA. Variation among the sizes for the various species may be due to differences in molecular weight, glycosylation patterns (Burton and Dwek, 2006), or mechanical flexibility (e.g., rotation of the Fabs, the arms of the Y, about the hinge region) of the antibody structures. We note that great care has been exercised here to dialyze the samples prior to analysis so that the peaks in Figure 1 represent exclusively antibodies (see Materials and Methods Section; Kaufman, 2000). These results indicate that antibodies in a solution can be in a monomeric or aggregated form.

The mobility size measured with ES-DMA can be compared with sizes obtained from protein crystallography. We recently demonstrated how to convert the projected areas, A_i , of DNA coated gold particles into the mobility size, d , accounting for Brownian motion that scrambles the orientation (Pease et al., 2007):

$$d = \left(\frac{\sqrt{\pi}}{6} \sum_{i=1}^3 A_i^{-1/2} \right)^{-1} \quad (2)$$

where A_i represents the projected area of the i th surface. Here, we examine two possible models for the IgG structure to determine the projected areas. The first model (Fig. 2a) assumes an IgG molecule to fill a solid rectangular “Y” with Fab-to-Fab and Fab-to-Fc (center-to-center) distances of 7–9 nm and 6–8 nm, respectively, from which we assume a width of 4.0 nm (Lee et al., 2002) and calculate Fab and Fc lengths to be 8.9 and 7.7 nm (Boehm et al., 1999). Equation (2) then predicts a size of 9.3 nm. The second model tunes the “Y” structure by utilizing the atomic coordinates of crystallographic structures found in the protein database for human IgG (Padlan, 1994; <http://www.umass.edu/microbio/rasmol/padlan.htm>, 2007). To calculate A_i , this model projects each atom in the human IgG structure into the

three views displayed in Figure 2b. Inserting the projected areas into Equation (2) yields a mobility size of 9.32 nm in excellent agreement with the 9.4 ± 0.2 nm size measured for human IgG. Therefore, the mobility size determined by ES-DMA is consistent with corresponding protein crystallographic structures.

The multiple peaks above 10 nm in Figure 1a and b are assigned to aggregates. Five or six peaks can be distinguished in Figure 1b, and Table I summarizes their sizes. We note that dimers could in principle form if two arbitrary antibodies were trapped in the same electrospray droplet. As the droplet dries, the two antibodies would be forced together, leading to the appearance of dimers in the spectra—a concern we address in detail below.

We apply the projected area models used to predict the sizes of the individual antibodies to identify each aggregate species. We assume a structure for aggregates that maximizes the contact area between antibodies where the “Y”-shaped antibodies are essentially stacked on top of each other. Thus the characteristic “Y” shape is conserved for aggregates with the only dimensional increase occurring in the direction normal to the plane defined by the “Y” shape of the antibody, that is, the thickness of the “Y” increases. Table I summarizes the predicted sizes. The close agreement between measured aggregate sizes (2nd column of Table I) and the model results (4th column) suggests that the model is also useful for predicting the size of protein aggregates in ES-DMA measurements.

Previously, Bacher et al. (2001), attempted to correlate empirically the mobility size (in nm) of a variety of biomolecular species from antibodies to viruses with their molecular weight (in kDa), using a model that assumes proteins to be globular spheres of constant density. Their empirical expression,

$$M_w = -22.033 + 9.830d - 1.247d^2 + 0.228d^3 \quad (3)$$

(which when solved for d becomes $d = 1.832M_w^{0.3256} \approx (6M_w/\pi\rho)^{1/3}$ where ρ is the density) is used to predict aggregates sizes in the last column of Table I. Comparison of

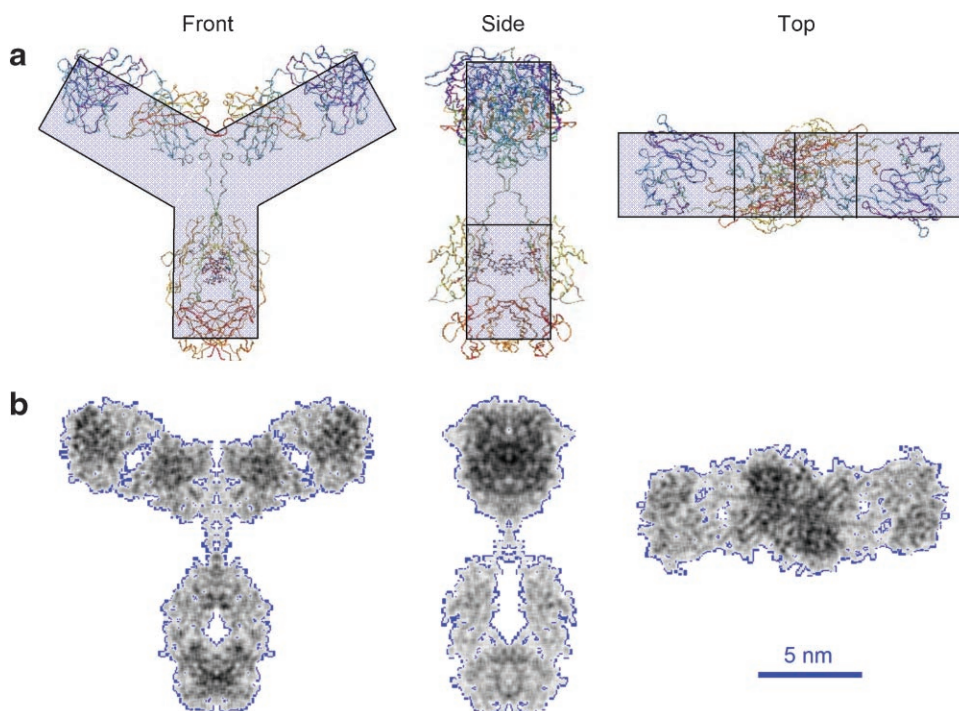


Figure 2. Front, side, and top views used to calculate the mobility size of human IgG (a) assuming the antibody fills a solid “Y” with Fab length of 8.9 nm (i.e., length of an arm of the Y), Fc length of 7.7 nm (i.e., the length of the stem of a Y), and width of 4.0 nm (Boehm et al., 1999) giving $A_{\text{front}} = 93.7 \text{ nm}^2$, $A_{\text{side}} = 53.1 \text{ nm}^2$, $A_{\text{top}} = 67.5 \text{ nm}^2$; and (b) from the protein crystallographic structure giving $A_{\text{front}} = 85.1 \text{ nm}^2$, $A_{\text{side}} = 65.8 \text{ nm}^2$, $A_{\text{top}} = 57.9 \text{ nm}^2$. The “Y” model in (a) is shown superimposed on a ribbon diagram obtained from the protein data bank. Darker grays in (b) represent greater atomic densities (Padlan, 1994, <http://www.umass.edu/microbio/rasmol/padlan.htm>, 2007).

the second and fifth columns shows that their empirical formula agrees reasonably well with the measured monomer, dimer, and trimer sizes.

Reversible (Physical) Aggregation

Several variables can affect the reversible aggregation of proteins including their concentration, the ionic strength of the buffer, pH, and electrospray droplet size. We now examine the role of each factor on the ES-DMA measurement.

Figure 3 shows the effect of increasing protein concentration from 18 to 370 $\mu\text{g}/\text{mL}$ on the proportion of dimers, trimers and higher-order aggregates in the rabbit IgG

solution as determined by ES-DMA. At the lowest concentration in Figure 3, 6% of the aggregates detected by ES-DMA are dimers. As the concentration increases the multimers detected substantially increase. With a 20-fold increase in antibody concentration, the multimers increase by 50%.

Although this apparent increase in aggregates with concentration could be due to concentration dependent aggregation, it must be considered, however, whether the distributions measured by ES-DMA are truly representative of the actual distributions in solution or if aggregates are formed inadvertently in the electrospray droplets as they dry. To examine the latter, we consider the probability of an electrosprayed droplet containing two or more antibodies.

Table I. Measured and calculated sizes for agglomerates in Figure 1b using structural models.

Number of antibodies	Measured size (nm)	“Y” shape calculated size (nm)	Protein data bank calculated size (nm)	Bacher et al., Mw correlated size (nm)
1/2	7.2	7.4	7.3	7.5
1	9.4	9.3	9.3	9.4
2	11.5	11.8	11.7	11.7
3	12.9	13.4	13.3	13.4
4	13.9	14.5	14.4	14.7
5	15.3	15.4	15.2	15.8
6	16.2	16.2	15.9	16.8

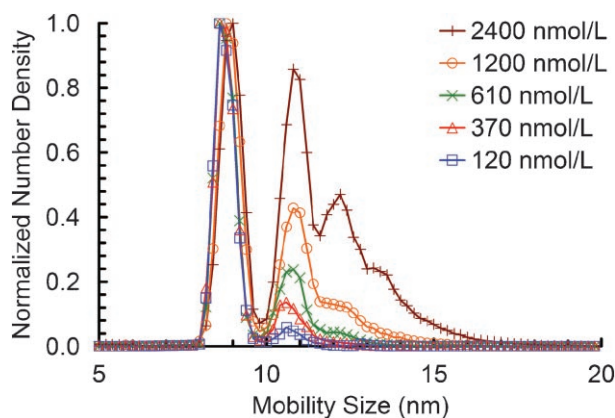


Figure 3. Number density normalized on the primary peak versus the mobility diameter of polyclonal rabbit antibodies at concentrations of 18 $\mu\text{g/mL}$ (120 nmol/L or 7.3×10^{13} antibodies/mL; blue \square), 55 $\mu\text{g/mL}$ (370 nmol/L or 2.2×10^{14} antibodies/mL; red \triangle), 91 $\mu\text{g/mL}$ (610 nmol/L or 3.7×10^{14} antibodies/mL; green \times), 180 $\mu\text{g/mL}$ (1.2 $\mu\text{mol/L}$ or 7.3×10^{14} antibodies/mL; orange \circ), and 370 $\mu\text{g/mL}$ (2.4 $\mu\text{mol/L}$ or 1.5×10^{15} antibodies/mL; brown $+$) each in 20 mmol/L ammonium acetate, pH 8. The total counts under the monomer peaks are 5.7×10^4 counts and 1.2×10^5 for the 120 and 370 nmol/L curves, respectively, and the total counts under the dimer peaks are 3.9×10^3 counts and 2.1×10^4 for the 120 and 370 nmol/L curves, respectively.

By performing ES-DMA on sucrose solutions, the diameter of a droplet was determined to be 150 nm, close to the 160 nm size reported by Kaufman (2000) under similar conditions. Assuming the protein to be uniformly distributed in solution, the concentration at which two antibodies will reside in the same droplet can be determined. Concentrations exceeding this cutoff value will lead to apparent dimers (or multimers) in the ES-DMA spectra, which do not exist in the original protein solution. The cutoff values in terms of the solution mass, molar, or number concentration (M_s , C_s , or N_s , respectively) are

$$M_s \ll \frac{6M_w}{\pi d_{\text{drop}}^3 N_A}, \quad C_s \ll \frac{6}{\pi d_{\text{drop}}^3 N_A}, \quad \text{or} \quad (4)$$

$$N_s \ll \frac{6}{\pi d_{\text{drop}}^3}$$

where N_A represents Avogadro's number, M_w is the molecular weight of an antibody (assumed to be 150 kg/mol herein), and d_{drop} is the droplet size as estimated from Kaufman (2000) or Lenggono et al. (2002). For a 150 nm droplet size, we find the cutoff to be 140 $\mu\text{g/mL}$ (940 nmol/L or 5.7×10^{14} antibodies/mL). Only the two highest concentrations in Figure 3 exceed this value. Apparent aggregation can occur at concentrations marginally below the cutoff concentration because the initial droplet sizes are not monodisperse, however the dimers detected at the lowest two concentrations in Figure 3 reflect real aggregates present in the sample solution.

The relative fraction of aggregates in the rabbit IgG sample decreases with concentration indicating reversible

aggregation. From the distributions in Figure 3 we can determine an equilibrium constant for the formation of dimers. The concentration of the monomers, C_1 , and dimers, C_2 , is related to the total number of counts under the monomer (8.0–9.8 nm) and dimer (10.0–11.6 nm) peaks, represented by N_1 and N_2 respectively, by

$$C_1 = \frac{N_1 C_{\text{tot}}}{N_1 + 2N_2} \quad \text{and} \quad C_2 = \frac{N_2 C_{\text{tot}}}{N_1 + 2N_2} \quad (5)$$

where C_{tot} is the total concentration monomer whether free or aggregated. The equilibrium constant can be extracted from the data using (Minton, 2007)

$$K_{\text{eq}} \equiv \frac{C_2}{C_1^2} = \frac{N_2(N_1 + 2N_2)}{N_1^2 C_{\text{tot}}} \quad (6)$$

Using values of N_1 , N_2 , and C_{tot} for the spectra in Figure 3, the equilibrium constant for the lower two concentrations in the figure is $K_{\text{eq}} = 6.3 \times 10^5 \text{ L/mol} \pm 4.6 \times 10^4 \text{ L/mol}$ (three standard deviations). This value is consistent with weakly associated proteins in the literature (Jimenez et al., 2007; Maynard and Georgiou, 2000; Minton, 2007; Mukkur and Smith, 1979).

To provide a concentration range over which ES-DMA can successfully analyze antibodies, we determined the lower limit of detection by plotting the intensity of the primary antibody peak versus solution concentration (data not shown) and then extrapolating the fitted curve of these data down to 10 counts, the noise floor for this instrument. With this approach, the lower limit of detection for antibodies in this size range is determined to be 180 ng/mL (1.2 nmol/L or 7.2×10^{11} antibodies/mL). We estimate the dynamic range for the study of IgG aggregation with ES-DMA to be approximately 180 ng/mL to 140 $\mu\text{g/mL}$, a concentration spanning nearly three orders of magnitude. The range is bounded on the lower end by the detection limit and at the upper end by droplet induced aggregation.

Figure 4 displays the effect of varying ammonium acetate concentration on ES-DMA spectra of IgG. As the concentration of ammonium acetate decreases at constant pH, aggregation appears to increase. The apparent aggregation cannot be explained by enhanced electrostatic attraction between like charged particles, because a decrease in ammonium acetate concentration (i.e., a decrease in the ionic strength) would be expected to accentuate electrostatic repulsion between the proteins, thereby decreasing the probability of dimer formation (Russel et al., 1989). A more likely explanation is that changes in ionic strength are affecting the size of electrosprayed droplets. Lenggono et al. (2002) reported that the diameter of electrosprayed droplets scales inversely with conductivity to the 1/3 power. Experimentally, we found the droplet diameter increases from 140 to 250 nm by decreasing the ionic strength from 20 to 2.0 mmol/L. Reducing the ionic strength effectively increases the drop size, thereby lowering the concentration cutoff by ~ 5 for the 10-fold change in ionic strength. Thus, the

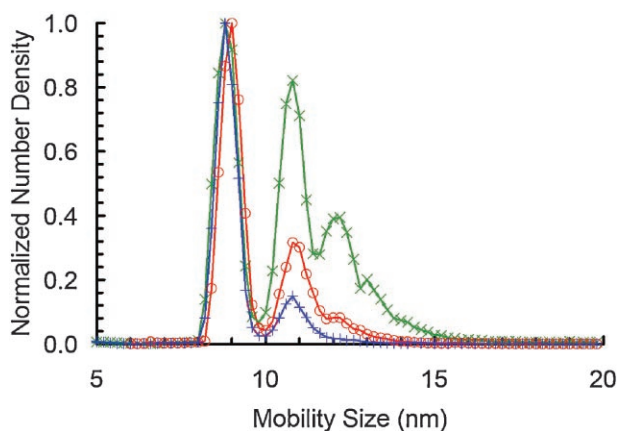


Figure 4. Number density versus the mobility diameter of polyclonal rabbit antibodies (55 $\mu\text{g/mL}$) at ammonium acetate concentrations of 2.0 mmol/L (green \times), 9.0 mmol/L (red \circ), and 20 mmol/L (blue $+$) ammonium acetate each at pH 8.

appearance of dimers and higher-order aggregates at the lower ionic strength in Figure 4 is because this spectrum was collected from a solution with an antibody concentration above the cutoff concentration (Eq. 4). This result indicates it is important to consider the effect of the ionic strength of the sample solution on droplet size when designing measurement protocols or comparing different protein solutions.

Chemically (Irreversible) Aggregation

A major concern in the biopharmaceutical industry is the ability to detect irreversible aggregates in antibody preparations, which can be responsible for immunogenic responses. To demonstrate the value of ES-DMA in analyzing irreversible aggregates, we examine the effect of two chemical crosslinkers on antibody aggregation.

Figures 5 and 6 show ES-DMA spectra of human IgG treated with two crosslinkers, paraformaldehyde and glutaraldehyde, respectively. Glutaraldehyde is considered to be a more effective crosslinking reagent than paraformaldehyde (Kiernan, 1999). We expect the proportion of larger clusters to increase with addition of crosslinker and with crosslinking efficacy. As seen in Figure 5, the addition of the slower crosslinker, paraformaldehyde, to the human IgG preparation only mildly aggregates the antibodies after 10 min. The dimeric and trimeric clusters increase relative to the control, and the tetramer and pentamer peaks become distinct.

ES-DMA spectra of antibodies treated with the more effective crosslinker, glutaraldehyde indicate more significant aggregation. Glutaraldehyde works by forming conjugated imines with the ϵ -amines of surface displayed lysines and can link together antibodies at multiple locations. In contrast to paraformaldehyde, however, the addition

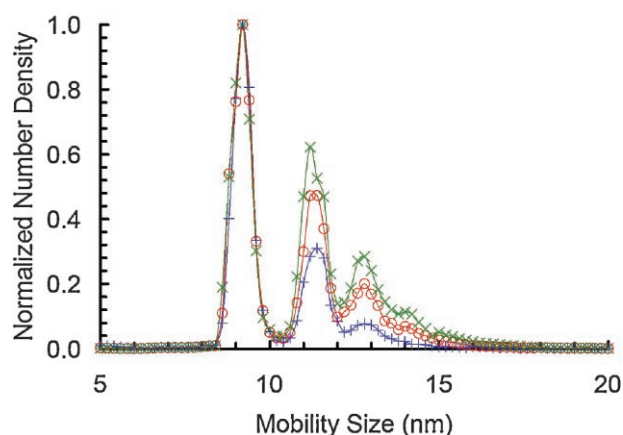


Figure 5. Number density normalized on the primary peak versus the mobility diameter of human IgG comparing a control (blue $+$) to additions of the crosslinker paraformaldehyde at 0.08% v/v (red \circ) and 0.8% v/v (green \times) each prepared in 2.0 mmol/L ammonium acetate at pH 8 and approximately 25 $\mu\text{g/mL}$ (170 nmol/L or 1.0×10^{14} antibodies/mL).

of glutaraldehyde results in the appearance of unresolved features at higher mobility sizes indicative of higher-order aggregates, suggesting more extensive crosslinking of antibodies. The number density at higher aggregate sizes continues to decay (inset Fig. 6) with a power law exponent of -1.86 . The magnitude of this exponent is reminiscent of the fractal dimension characteristic of diffusion limited cluster-cluster aggregation for colloids, which is typically ~ 1.7 – 1.8 (Larson, 1999). This interpretation is consistent with the well known reactivity of glutaraldehyde in which

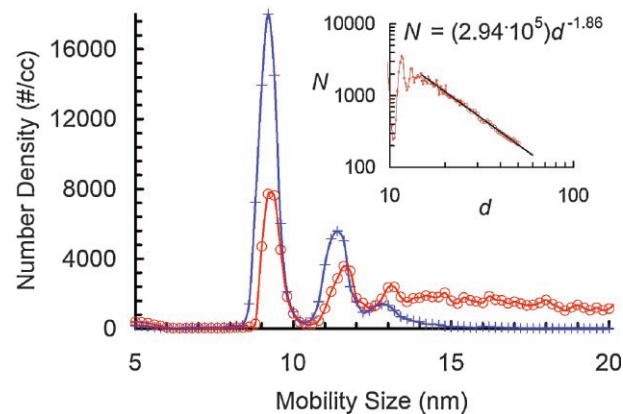


Figure 6. Number density versus the mobility diameter of human IgG comparing a control (blue $+$) to additions of the crosslinker glutaraldehyde at 0.14% v/v (red \circ) prepared in 2.0 mmol/L ammonium acetate at pH 8 and approximately 25 $\mu\text{g/mL}$ (170 nmol/L or 1.0×10^{14} antibodies/mL). The inset is a log-log plot of the number density, N , exhibiting a power law decay with an exponent of -1.86 . Higher glutaraldehyde concentrations (1.4% v/v) resulted in rapid clogging of the silica capillary used for electrospray. Accordingly, we believe the IgG agglomerated to the extent that the aggregates failed to transit the capillary, blocking instead its flow.

Table II. Percentage of aggregates from numerically summing the counts under the peaks.

	Monomer (%)	Dimer (%)	Trimer (%)	Tetramer (%)	Pentamer (%)	Higher order (%)
Control	56.8	28.5	9.7	2.3	1.3	1.5
Formaldehyde 0.08%	43.2	29.4	19.7	5.8	0.9	1.0
Formaldehyde 0.80%	33.9	30.6	22.4	6.9	3.6	2.5
Gluteraldehyde 0.14%	7.2	5.6	4.0	2.8	3.1	77.4

Table III. Comparison widely used methods to determine protein aggregation.

Technique	Advantages	Disadvantages
SEC	Widely used in biotech industry, fast (<1 h)	Matrix interactions can alter aggregate distributions and complicate quantitation and sizing, mobile phase usually different from formulation buffer
DLS	Fast (<1 h), high sensitivity for large aggregates, potential for measuring aggregate distributions in formulation buffer, no matrix interactions	Difficult to resolve small aggregates from monomer, obtaining aggregate size distribution requires fitting of correlation function
AUC	Quantifiable, potential for measuring aggregate distributions in formulation buffer, no matrix interactions	Slow (~day), expensive, obtaining aggregate size distributions requires fitting of sedimentation profiles
ES-DMA	Provides direct, quantitative read-out of aggregate distributions, fast (<1 h), well suited for studying early stages of aggregation	Limited concentration range, electrospray buffer different from formulation buffer, not currently used in biotech industry

Brownian diffusion is the rate limiting step in cluster–cluster formation. More importantly, the inset to Figure 6 shows that aggregates of significant size can be measured with ES-DMA. Although our data extends to 50 nm, extrapolating the fit down to 10 counts suggests that aggregates as large as 250 nm can be observed. Higher gluteraldehyde concentrations (1.4% v/v) resulted in rapid clogging of the silica capillary used for electrospray. Accordingly, we believe the IgG agglomerated to the extent that the aggregates failed to transit the capillary, blocking instead its flow.

The amount of aggregation depicted in Figures 5 and 6 is summarized in Table II. Each entry represents the sum of all the number densities or counts under each peak divided by total counts for all the peaks. As expected, as the strength of the crosslinker increases, the proportion of monomer and dimer tends to decrease relative to the control, while the higher-order aggregates increase substantially. Indeed, with gluteraldehyde, the larger aggregates represent over 77% of the population as expected for this aggressive crosslinker. This result indicates ES-DMA to be valuable for detecting small to moderately sized aggregates, which may be more difficult to detect and quantify with other techniques.

Conclusions

In summary, we can compare ES-DMA for measuring protein aggregation to the most widely used analytical methods, including size exclusion chromatography (SEC), dynamic light scattering (DLS), and analytical ultracentrifugation (AUC). We summarize the advantages and disadvantages of each along with ES-DMA in Table III. We refer the reader to the work by Bondos (2006) and others (Gabrielson et al., 2007; Wang, 2005) who offer more

extensive comparison of the most widely used methods to measure protein aggregation.

The primary advantages of ES-DMA for measuring protein aggregation include characterization of species with molecular weights exceeding 10 kDa (especially for species >250 kDa), high resolution needed to distinguish dimers from trimers and tetramers, direct determination of the aggregate's aerodynamic size, and quantitative determination of the proportion of each aggregate species for both chemically crosslinked and self-associated antibodies. The primary limitation of the method is the limited concentration range (180 ng/mL to 140 µg/mL) and the current inability to examine proteins in formulation buffers (nonvolatile salts coat the proteins and obscure the distribution). It may be possible to extend the upper concentration range (up to 5 mg/mL) by using smaller diameter capillaries (e.g., 10 µm i.d. as in nanoelectrospray), which would produce smaller droplets (Feng and Smith, 2000).

LFP would like to acknowledge support of a postdoctoral fellowship through the National Research Council and helpful discussions with Rebecca A. Zangmeister.

References

- Attri AK, Minton AP. 2005. New methods for measuring macromolecular interactions in solution via static light scattering: Basic methodology, and application to nonassociating and self-associating proteins. *Anal Biochem* 337(1):103–110.
- Bacher G, Szymanski WW, Kaufman SL, Zollner P, Blaas D, Allmaier G. 2001. Charge-reduced nano electrospray ionization combined with differential mobility analysis of peptides, proteins, glycoproteins, non-covalent protein complexes and viruses. *J Mass Spectrom* 36(9):1038–1052.

- Boehm MK, Woof JM, Kerr MA, Perkins SJ. 1999. The Fab and Fc fragments of IgA1 exhibit a different arrangement from that in IgG: A study by X-ray and neutron solution scattering and homology modelling. *J Mol Biol* 286(5):1421–1447.
- Bondos SE. 2006. Methods for measuring protein aggregation. *Curr Anal Chem* 2(2):157–170.
- Braun A, Kwee L, Labow MA, Alsenz J. 1997. Protein aggregates seem to play a key role among the parameters influencing the antigenicity of interferon alpha (IFN-alpha) in normal and transgenic mice. *Pharm Res* 14(10):1472–1478.
- Burton DR, Dwek RA. 2006. Immunology—Sugar determines antibody activity. *Science* 313(5787):627–628.
- Demeule B, Lawrence MJ, Drake AF, Gurny R, Arvinte T. 2007. Characterization of protein aggregation: The case of a therapeutic immunoglobulin. *Biochim Biophys Acta—Proteins Proteomics* 1774(1):146–153.
- Feng BB, Smith RD. 2000. A simple nanoelectrospray arrangement with controllable flowrate for mass analysis of submicroliter protein samples. *J Am Soc Mass Spectrom* 11(1):94–99.
- Frokjaer S, Otzen DE. 2005. Protein drug stability: A formulation challenge. *Nat Rev Drug Discov* 4(4):298–306.
- Gabrielson JP, Brader ML, Pekar AH, Mathis KB, Winter G, Carpenter JF, Randolph TW. 2007. Quantitation of aggregate levels in a recombinant humanized monoclonal antibody formulation by size-exclusion chromatography, asymmetrical flow field flow fractionation, and sedimentation velocity. *J Pharm Sci* 96(2):268–279.
- Hermeling S, Crommelin DJA, Schellekens H, Jiskoot W. 2004. Structure-immunogenicity relationships of therapeutic proteins. *Pharm Res* 21(6):897–903.
- Jimenez M, Rivas G, Minton AP. 2007. Quantitative characterization of weak self-association in concentrated solutions of immunoglobulin G via the measurement of sedimentation equilibrium and osmotic pressure. *Biochemistry* 46(28):8373–8378.
- Kaufman SL. 2000. Electrospray diagnostics performed by using sucrose and proteins in the gas-phase electrophoretic mobility molecular analyzer (GEMMA). *Anal Chim Acta* 406(1):3–10.
- Kiernan JA. 1999. *Histological and histochemical methods*. Oxford: Butterworth/Heinemann.
- Knutson EO, Whitby KT. 1975. Aerosol classification by electric mobility: Apparatus, theory, and applications. *J Aerosol Sci* 6:443–451.
- Larson RG. 1999. *The structure and rheology of complex fluids*. New York: Oxford University Press. 331 p.
- Lee KB, Park SJ, Mirkin CA, Smith JC, Mrksich M. 2002. Protein nanoarrays generated by dip-pen nanolithography. *Science* 295(5560):1702–1705.
- Lenggoro IW, Xia B, Okuyama K, de la Mora JF. 2002. Sizing of colloidal nanoparticles by electrospray and differential mobility analyzer methods. *Langmuir* 18(12):4584–4591.
- Loo JA. 1997. Studying noncovalent protein complexes by electrospray ionization mass spectrometry. *Mass Spectrom Rev* 16(1):1–23.
- Mauro M, Craparo EF, Podesta A, Bulone D, Carrotta R, Martorana V, Tiana G, San Biagio PL. 2007. Kinetics of different processes in human insulin amyloid formation. *J Mol Biol* 366(1):258–274.
- Maynard J, Georgiou G. 2000. Antibody engineering. *Annu Rev Biomed Eng* 2:339–376.
- Minton AP. 2007. Static light scattering from concentrated protein solutions, I: General theory for protein mixtures and application to self-associating proteins. *Biophys J* 93:1321–1328.
- Mukkur TKS, Smith GD. 1979. Self-association of bovine immunoglobulin-G1. *Biochem J* 183(2):463–465.
- Mulholland GW, Donnelly MK, Hagwood CR, Kukuck SR, Hackley VA, Pui DYH. 2006. Measurement of 100 nm and 60 nm particle standards by differential mobility analysis. *J Res Natl Inst Stand Technol* 111(4):257–312.
- Padlan EA. 1994. Anatomy of the antibody molecule. *Mol Immunol* 31(3):169–217.
- Pease LF, Tsai D-H, Zangmeister RA, Zachariah MR, Tarlov MJ. 2007. Quantifying the surface coverage of conjugate molecules on functionalized nanoparticles. *J Phys Chem C* 111(46):17155–17157.
- Russel WB, Saville DA, Schowalter WR. 1989. *Colloidal dispersions*. Cambridge, UK: Cambridge University Press.
- Treuheit MJ, Kosky AA, Brems DN. 2002. Inverse relationship of protein concentration and aggregation. *Pharm Res* 19(4):511–516.
- Wang W. 2005. Protein aggregation and its inhibition in biopharmaceutics. *Int J Pharm* 289(1–2):1–30.
- Wiedensohler A. 1988. An approximation of the bipolar charge-distribution for particles in the sub-micron size range. *J Aerosol Sci* 19(3):387–389.